Journal of Materials Chemistry B

RSC Publishing

PAPER

View Article Online
View Journal | View Issue

Cite this: J. Mater. Chem. B, 2013, 1, 6094

Probing the interactions of chitosan capped CdS quantum dots with pathogenic bacteria and their biosensing application†

Hani Nasser Abdelhamid[ab] and Hui-Fen Wu*[acde]

Chitosan modified CdS quantum dots (CdS@CTS) can be used as an effective bacterial biosensor due to their good bioaffinity among chitosan molecules and bacterial membranes. CdS@CTS is an ultrafast, sensitive, direct and biocompatible biosensor for pathogenic bacteria (*Pseudomonas aeruginosa* and *Staphylococcus aureus*). Chitosan biopolymer of CdS@CTS provides bioaffinity sites that can be employed for the assembly on pathogen bacteria cells due to the chemical similarity of the chitosan and the bacteria membranes. Thus, *S. aureus* and *P. aeruginosa* cells were detected at low concentrations of 150 and 200 cfu mL^{-1}, respectively, in an extremely short time (1 min). The CdS@CTS–bacteria interaction is noncovalent. From the thermodynamic results, the van der Waals force and hydrogen bonding formation are characterized by negative enthalpy (ΔH), while positive entropy (ΔS) is considered as the evidence for typical hydrophobic interactions. Moreover, negative ΔH and positive ΔS might play a role in the electrostatic interactions. The negative free energy (ΔG) shows that the binding events were spontaneous processes. Matrix assisted laser desorption/ionization mass spectrometry (MALDI-MS) and transmission electron microscopy (TEM) were performed to evaluate the interactions and the biocompatibility of CdS@CTS toward bacteria cells. Their biocompatibility, together with the high sensitivity and the presence of multifunctional forces, making these quantum dots (CdS@CTS) an excellent and novel biosensor which can be widely applied in the near future.

Received 24th July 2013
Accepted 4th September 2013

DOI: 10.1039/c3tb21020k

www.rsc.org/MaterialsB

Introduction

Quantum dots (QDs) are nanomaterials with distinct optical and electronic properties.[1] They have high photostability and so are more applicable than conventional dyes.[2–6] Moreover, the emission of QDs fluorescence is about 20 times brighter than conventional fluorescent dyes.[7] QDs are almost the same size as biomolecules, so they are useful to serve as effective biosensors.[8–11] The photoluminescence (PL) property of QDs is strongly dependent on the nature of the surface of the capping agents.[12,13] Interactions among the biomolecules and the QDs surfaces could mainly result in changes of PL efficiency,[14–18] so it has been intensively used for biosensing.

Bacterial pathogens are distributed everywhere, such as soil, marine water, and contaminated water. The methods of test bacteria meet a number of challenges. Time and sensitivity are the most important limitations of microbiological analysis.[19–23] Due to the great photostability of quantum dots (QDs), they can be used for imaging cell surfaces.[24] Generally, semiconductor QDs can reduce the autofluorescence of plague cells because QDs have longer fluorescence lifetimes than the cell autofluorescence. Thus, it can drastically reduce the common background signals which are emitted from the biological samples. Furthermore, QDs emission is independent of excitation wavelength,[25] so that samples can be stained with QDs and we can use lower energies of laser (using high excitation wavelength) than the autofluorescence. That can be also adjusted by controlling the QDs particle sizes.[26–29] Furthermore, the high brightness of QDs increases the sensitivity for fluorescence assays.[30–37] Thus, quantum dots coated with antibody were proposed for bacteria detection and biosensing.[38–42] The antibody-QD (also called immune-QD) probe has demonstrated good selectivity for surface bacteria,[43–46] although it is expensive and inhibits the cell growth. Further, most antibody-QDs are instable due to aggregation in short time and require lengthy processing steps for synthesis; so the performance is limited by sample pH and they are size dependent for QDs.[38–42] Generally, quantitative analysis by fluorescence is challenging due to

[a]Department of Chemistry, National Sun Yat-Sen University, Kaohsiung, 804, Taiwan. E-mail: hwu@faculty.nsysu.edu.tw; Fax: +886-7-525-3908; Tel: +886-7-5252000-3955
[b]Department of Chemistry, Assuit University, Assuit, 71516, Egypt
[c]Center for Nanoscience and Nanotechnology, National Sun Yat-Sen University, Kaohsiung, 804, Taiwan
[d]Doctoral Degree Program in Marine Biotechnology, National Sun Yat-Sen University, Kaohsiung, 804, Taiwan
[e]School of Pharmacy, College of Pharmacy, Kaohsiung Medical University, Kaohsiung, 806, Taiwan

† Electronic supplementary information (ESI) available. See DOI: 10.1039/c3tb21020k

the signals variations especially for complex bacteria studies.[47–50] Therefore, new biosensors with strong bioaffinity toward bacteria, are necessary to be developed.[50] Chitosan is a linear β-1,4-linked polysaccharide that is obtained by the partial deacetylation of chitins. Applications of chitosan are reviewed in ref. 51. The chemical structures of the biopolymers are similar to those of the bacteria membranes; thus they have great affinity toward bacteria cell membranes. Besides, the quantum dots can be easily modified with chitosan which possesses many coordination sites.[52]

In this work, we aimed to design and prepare novel chitosan modified quantum dots (CdS@CTS) that can be effectively applied for biosensing pathogenic bacteria. We also attempt to probe the interaction forces among chitosan biomolecules and the pathogenic bacteria membranes *via* thermodynamic studies. Two different pathogenic bacteria "*Pseudomonas aeruginosa* and *Staphylococcus aureus*" are investigated. The cytotoxicity of CdS@CTS was recorded using the plate counting method, and optical density (OD_{600}). Amoxicillin and quantum dots modified mercaptoproponic acids (MPA) were used as the contrast samples. Thermodynamic analysis of the interactions among the pathogenic bacteria and the CdS@CTS QDs reveal that the interactions are spontaneous and were driven entropically. The interactions of bacteria cell membranes with quantum dots were investigated using transmission electron microscopy (TEM) and matrix assisted laser desorption/ionization mass spectrometry (MALDI-MS).

Materials and method

Materials

Chitosan (low molecular weight; 50 000–190 000 g mol^{-1}), 75–85% de-acetylation, sodium sulfide, glacial acetic acid, cadmium nitrate (99.0%), mercaptoproponic acid (MPA) and ammonium hydroxide were purchased from Sigma-Aldrich, Australia. The de-ionized water was obtained from Milli-Q Plus water purification system (Millipore, Bedford, MA, USA).

Apparatus

The fluorescence measurements were made using F-2700 fluorescence spectrophotometer (Hitachi Co.), which was equipped with a xenon lamp (150 W), a recorder, dual monochromators and a quartz cell (1 × 1 cm). The absorption spectra were acquired on U-3501 spectrophotometer (Hitachi Corporation, Japan). Fourier transform infrared (FT-IR) spectra of quantum dots were recorded on Spectrum 100, Perkin Elmer, USA. Transmission electron microscopy (TEM, Philips, CM200) was used for quantum dots characterization. For TEM analysis, colloidal solutions of the quantum dots in water were dropped on the 50 Å thick copper grids and wicked away the excessive solution immediately. pH value was adjusted using istek 72OP.

Synthesis of CdS quantum dots capped with MPA

CdS quantum dots were prepared as mentioned previously.[53] Briefly, 400 μL of 3-MPA was transferred into a round bottom flask (250 mL) containing 15 mL of deionized water. About 2 mL of cadmium nitrate solution (10 mM) was added dropwise to the previous solution under N_2 pressure with constant stirring for 1 h. The pH of the solution was adjusted to be 9 by adding ammonium hydroxide solution (37%). Sodium sulfide solution (2.5 mL, 8 mM) was quickly added to the above solution at 96 °C with continuous stirring for 2 h. The obtained clean green yellowish CdS QDs solution was stored at 4 °C until further use.

Synthesis of chitosan modified CdS QDs

The synthesis procedure of chitosan modified CdS QDs was modified from previous literature reports[54] as in Scheme S1.† Chitosan solution was prepared by dissolving 0.1 g in 20 mL with 1% acetic acid. Then, the solution was mixed with 11 mg cadmium nitrate and subjected to continuous stirring for 24 h to facilitate chelating of Cd^{2+} with chitosan. The solution has been purged with pure nitrogen gas for at least 30 min under magnetic stirring. Then, solution of $Na_2S{\cdot}9H_2O$ (12 mg, 10 mL H_2O) was dropped slowly into the mixed solution. Finally, the colloidal solution was sealed and incubated for 5 h at 35 °C. The colloid solution was stored at room temperature without any evidence of precipitation for more than one month.

Bacteria cultivation

Both bacteria were cultivated using conventional methods. *Staphylococcus aureus* (BCRC 10451) and *Pseudomonas aeruginosa* (BCRC 10303) standard cultures were purchased from Bioresource Collection and Research Center (Hsin-Chu, Taiwan). The subculture of both bacteria was published in detail in ref. 55. The bacterial cultures were stored in powdered solid-phase (lyophilized). About 0.1–0.2 mL of the bacteria culture was streaked directly onto an appropriate agar plate and incubated at 37 °C. The bacteria were cultured repeatedly into fresh medium every two days for a week (sub-culturing) before use. Sub-culture after growth on agar plate, it re-suspended in sterilized de-ionized water for all experiment.

Spectroscopy methods

Bacterial biosensing. After bacteria growth (24 h), it was carefully re-suspended immediately prior to acquisition of emission spectra. Simply, a Petri dish of freshly cultured *S. aureus* and *P. aeruginosa* were scraped from the surface of agar plate and suspended in 1 mL of deionized water. From the previous suspension, different volumes contain bacteria cells (5×10^2, 1×10^3, 1.5×10^3, 2.0×10^3, 2.5×10^3, 3×10^3, 3.5×10^3, … , 1×10^{10} cfu 10 μL^{-1}) are added to 1 mL of CdS@chitosan (100 μg mL^{-1}). Cell numbers were counted in the final volume, *i.e.*, 1 mL using plate counting protocol.

In order to optimize the parameters such as excitation wavelength, QDs concentration, and contact time, we investigated each parameter separately. CdS@CTS was excited with a broad excitation wavelength, *i.e.*, 285, 295, 305, 320, 330, 340, 350, 360, 370, 380, 390, and 400 nm. To optimize CdS@CTS concentration, at wavelength 295 nm, different concentrations of CdS@CTS (25, 30, 50, 60, 100, 200, 300, 400, 500, and 600 μg mL^{-1}) were investigated. Contact time was optimized *via* incubation

CdS@CTS (100 μg mL^{-1}) with *P. aeruginosa* (1×10^3 cfu mL^{-1}) and emission was recorded in intervals, *i.e.*, 1, 2, 3, 5, 7, 10, 12, and 15 min.

Plate count protocol. The number of target organisms present in the sample (1 mL) was determined by surface plating 0.01 mL of *P. aeruginosa* and *S. aureus* dilutions on agar (Difco Laboratories). After incubating at 37 °C for 24 h; the presence of the organisms was confirmed by the color of the colonies on the media; *S. aureus* was golden; while *P. aeruginosa* was blue-green on agar.

Cell viability. The cell viability of the two bacteria was measured using optical density after incubation at 10 min. The optical density (OD_{600}) of the two different bacteria was measured at $\lambda_{max} = 600$ nm using UV-vis spectroscopy.

Matrix assisted laser desorption/ionization mass spectrometry (MALDI-MS) measurements. In order to measure the interactions of bacteria with quantum dots (CdS@MPA and CdS@CTS), about 10 μL of bacteria suspension were mixed with 10 μL of quantum dots and incubated for 10 min. Then, 10 μL of sinapinic acid matrix (50 mM, 50 : 50 aqueous acetonitrile) were added. About 2 μL of the mixture were spotted on the MALDI plate and then we waited for drying before analysis.

Transmission electron microscopy (TEM). To visualize the morphology change of the tested bacteria, TEM images were recorded. In typical procedures, bacteria cells (1 mL, 10^4 to 10^5 cfu mL^{-1}) were treated with quantum dots (100 μL) and then were suspended for 30 min with 2.5% glutaraldehyde. The cells were washed with de-ionized water and then post-fixed with 1% aqueous OsO_4 (Fluka) for 30 min and then washed again twice with water. 10 μL of the mixture were placed on the copper grids and then dried for TEM measurements.

Results and discussion

For biosensing studies, the luminescent probes based on quantum dots are more attractive compared with the conventional organic dyes. The main reasons are due to the spectroscopic properties of QDs that match the needs of biological uses, such as long fluorescence lifetimes, large apparent Stokes shifts, and can be tuned to achieve high fluorescence emission. Moreover, the QDs suffer from poor solubility and high cytotoxicity. To circumvent these limitations, chitosan modified CdS was prepared. Chitosan is biocompatible biopolymers that can improve the solubility and decrease the cytotoxicity of xenobiotic elements such cadmium ions due to the high coordination.

Characterization of quantum dots

TEM image (Fig. 1A) was used to determine the size and the morphology of CdS@CTS. The predominant size was about 3.33 nm based on the number of particles (see inset of Fig. 1A). According to the empirical equation (1),[27] the size of nanoparticles is 3.38 nm, which is in agreement with the size of TEM image.

$$D = (-6.6521 \times 10^{-8})\lambda^3 + (1.9557 \times 10^{-4})\lambda^2 - (9.2352 \times 10^{-2})\lambda + (13.29) \quad (1)$$

where, D (nm) is the size of a given nanocrystal sample, and λ (nm) is the wavelength of the first excitonic absorption of the corresponding sample (Fig. S1(A) of ESI†).

The size of CdS@CTS was also confirmed from the UV spectra in Fig. S1(A).† The absorption spectrum indicates that the CdS@CTS had a red shifted absorption onset relative to CdS@MPA, owing to the capping agent. Based on the extinction coefficient measurement,[56] the CdS@CTS offers the same size (3.38 nm) which is completely in agreement with the TEM results and the eqn (1) values. TEM image (Fig. S1(B), ESI†) of the CdS@MPA shows mainly the same size, *i.e.*, 3 nm. FT-IR spectra (Fig. S1(C), ESI†) of pure chitosan displays transmissions at 1588, and 1074 cm^{-1} corresponding to the amide II band, and the –C–O–C– vibration, respectively.[57] However, the CdS shifts amide II bands of chitosan noticeably from 1588 to 1543 cm^{-1}. The hydroxyl group (a broad band) at 3300 cm^{-1} of the free chitosan appears sharper in the CdS@CTS QDs due to the hydrogen bonds with the quantum dots. Peaks at 2900–2800 cm^{-1} are corresponding to C–H vibrations. FTIR spectra reveal that the CdS QDs have produced a strong complex with chitosan biopolymer (Fig. S1(C), ESI†). The strong interaction is due to presence of high coordinating functional groups such as amine ($-NH_2$), hydroxyl (–OH) and carboxylic groups (–COOH).[58] Quantum dots (CdS) at excitation wavelength 295 nm ($\lambda_{ex} = 295$ nm), offers an emission peak (Fig. 1B) centered at 590 nm, which is the typical luminescence of CdS nanocrystals resulting from the transition of electrons from shallow states near the conduction band to sulfur vacancies present near the valence band. Fig. 1C shows that the excitation wavelength (295 nm) exhibits high emission intensity of QDs. In order to apply quantum dots for effective biosensing studies, the QDs should have the following features including excellent stability, fast response to bacteria, biocompatible, and display photoluminescence changes with bacteria cell additions. These important parameters were investigated for effective quantum dots applied for pathogenic bacteria biosensing and are presented below.

Stability of the CdS@CTS QDs

Stability of nanoparticles is of paramount concern. The stability of nanoparticles depends mainly on the capping or stabilizing agents which were used during the preparation steps. QDs capped with small molecules like mercaptoproponic acid (MPA) are easily degraded by hydrolysis or oxidation on the capping ligands.[25,30,59–61] The mercaptoproponic acid modified QDs are not completely stable. It displays slow desorption of mercaptoacetic acid molecules from the surface of QDs that results in aggregation and precipitation for the QDs.[62] In contrast, the CdS@CTS QDs exhibit excellent stability for a long time (about one month) without any aggregation. The excellent stability can be confirmed from the fluorescence emissions (Fig. 1D) which show no changes/shifts in the fluorescence peaks.[63,64] Chitosan forms a stable colloidal solution without any record of degradation (Fig. 1B). Further, it is a photostable compound, while thiols (such as MPA) can undergo oxidation by lights to form dimmers. The dimerization reaction has high probability when thiols interact with laser radiation during excitation.[65]

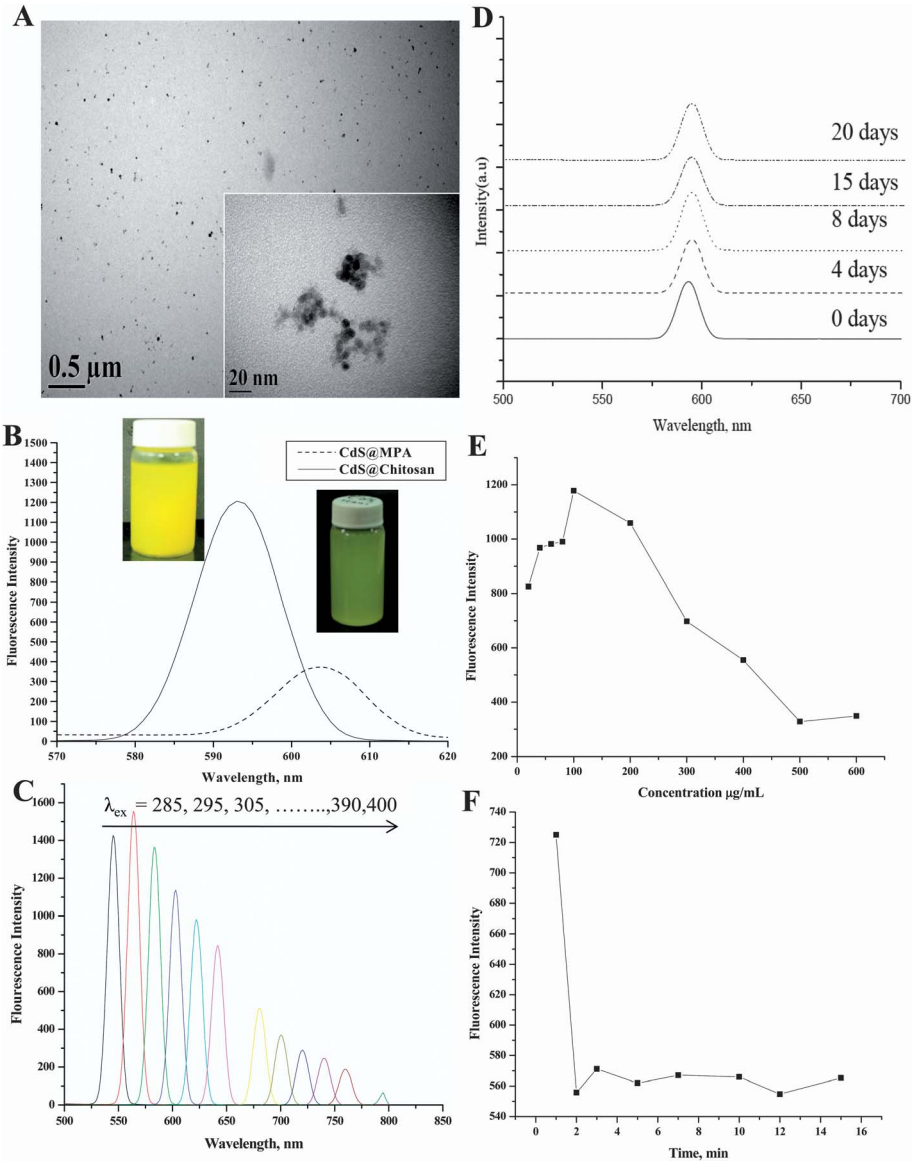

Fig. 1 Characterizations of CdS@CTS system using (A) TEM, (B) fluorescence, (C) excitation of CdS@CTS with different excitation wavelength, (D) stability of fluorescence emission, (E) effect of concentration on QDs emission, and (F) contact time of bacteria–QDs interactions.

Optimization of the biosensor concentration and contact time

Prior to using quantum dots as a biosensor, there are influential factors such as contact time and concentration should be optimized to achieve high sensitivity. The first requirement to build a QD biosensor is the changes of quantum dot intensity upon addition of the bacteria cells in order to observe the influence on the bacteria cell numbers. In Fig. 1E, the experimental results indicate that the fluorescence intensity was significantly increased with the increase of the CdS@CTS QD concentration. Fig. 1E shows the increase of fluorescence intensity reaches the maximum with concentration of 100 μg mL^{-1} after that the intensity dramatically decreases. The optimized concentration, *i.e.*, 100 μg mL^{-1} is used in further studies. A decrease of intensity at high concentration (>100 μg mL^{-1}) may be due to self-quenching or self-absorption. This concentration is considered to be very low if compared with CdSe QDs modified with small molecules (such as thioglycolic acid, TGA, 1 mg mL^{-1}) that was proposed to detect bacteria by binding covalently to bacteria cells using chemistry cross-linking (1-ethyl-3-(3-dimethylaminopropyl) carbodiimide (EDC)).[40]

Generally, the biosensor should have fast response time on the addition of the target analytes. These responses depend on the interaction modes between the analytes and nanomaterials. If the interactions among the bacteria cell membranes and QDs are strong, it will cause momentary changes on the QDs fluorescence. Fig. 1F reveals 1 min of contact time is ideal to perform the measurements and to achieve the steady state of fluorescence intensity. In contrast with the conventional techniques,[19–23] the CdS@CTS offers fast response due to the non-covalent interactions among chitosan and bacteria membranes. Decrease of the intensity after 1 min, may be due to the strong

interactions between the bacteria with the CdS@CTS QDs, resulting from formation of sediments to quench the signals. Similar observation has been reported when graphene functionalized with Fe_3O_4@chitosan was used for bacteria biosensing.[50] The situation is quite different as QDs are lighter materials over than graphene and magnetic nanoparticles. This observation reveals the aggregation of QDs on the surfaces of bacteria membranes.

Biocompatibility of CdS@MPA and CdS@CTS QDs

The cytotoxicity of quantum dots is important and should be investigated. To apply quantum dots for biological application, the biocompatibility is required. The cytotoxicity of quantum dots limits their applications. Thus, a new class of quantum dots without cadmium has been proposed and was named as "cadmium free quantum dots". The toxicity of quantum dots typically originates from two main sources: the core of quantum dots and the capping agents. Degradation of the molecules coated on the QDs is the main reason for QDs cytotoxicity. Some coating materials on the QDs have been found to be cytotoxic, such as mercapto-acid.[66,67] The QDs toxicity has been attributed to oxidative or photolytic degradation of the core coatings of QDs.[66] Cytotoxicity also may be from the free cadmium ions in solution.[68] These xenotoxic elements can bind to genome or other biomolecules and cause cell death. For instance, CdS@MPA causes quantitative degradation of extracellular polysaccharides (EPS) of *Escherichia coli*.[69] To investigate the cell viability of CdS@CTS against the two pathogenic bacteria, the optical density method was used and the optical density (OD_{600}) was measured at 600 nm. The method is based on the turbidity measurements which give signals corresponding to the bacteria cell numbers. To evaluate the cytotoxicity of CdS@CTS, amoxicillin and CdS@MPA were used as contrast agents. Fig. 2A of *P. aeruginosa* and Fig. 2B of *S. aureus* exhibit lower toxicity to CdS@CTS over that of the CdS@MPA and the reason is due to better biocompatibility of coating agent and strong chelating of Cd core with chitosan. However, the yeast cells (*Saccharomyces cerevisiae*) have been used as a simple and efficient biosynthesis method to prepare easily harvested biocompatible cadmium telluride (CdTe) quantum dots (QDs).[70]

In order to understand these conundrums, more parameters should be considered as reviewed in ref. 71 such as types of capping agent, agents stereochemistry, toxicity of QDs cores, types of pathogenic bacteria, and the analytical techniques that applied to probe the cytotoxicity of nanomaterials. Derfus *et al.*[68] reported in-depth investigation of CdSe quantum dots with different coatings in hepatocytes. They reported that the liberation of cadmium ions is the main reason of QDs cytotoxicity.[68] So that large biomolecules or strong coordinating agents such as chitosan may prevent free cadmium ions. Capping agents also may cause toxicity toward the cells. However, thiols used as capping agents were found to be non-toxic if they were kept in an inert atmosphere, but when exposed to air, it can be degradable and oxidized very easily. Thus, cadmium ion can be released. Li *et al.*[72] observed that QDs coated with d-GSH (d form of glutathione, the non-biologically active form of GSH) showed less cytotoxicity than l-GSH-coated QDs. That indicates stereochemistry has influence on the cytotoxicity of QDs.[72] Also, we should note that these studies investigated different bacteria which surely have a different response towards QDs. To ensure the biocompatibility of the introduced system, plate counting was reported. Data (Fig. S2†) show sharp decreases in bacteria number in the case of CdS@MPA over CdS@CTS. The optical density (OD_{600}) and plate counting results (Fig. S2†) support the biocompatibility of CdS@CTS QDs. Recently, alginate–chitosan multilayers were deposited onto alginate matrices as an effective strategy for the encapsulation of probiotic bacteria which can be protected at low pH.[73] However, chitosan was proposed as antibacterial agents after modified as Schiff base[74] or capping with ZnO.[75]

Application of CdS@CTS QDs as a feasible biosensor

Detection of the low numbers of bacteria cells represents the ultimate level and the longstanding goal of biosensing. To serve as an effective biosensor, the biomaterials should display photoluminescence change (quenching, enhancement or peak shifts "ratiometric biosensor") upon addition of different numbers of the pathogenic bacteria. As shown in Fig. 2C (*P. aeruginosa*) and Fig. 2D (*S. aureus*), there are increases of fluorescence intensity upon addition of different colony forming unit cfu mL^{-1}. The prime reason for the fluorescence enhancement is due to the aggregation of QDs on the bacteria membranes which induce enhancement "aggregation induced emission enhancement, AIEE". Under the optimum conditions (at 100 μg mL^{-1}, $\lambda_{ex} = 295$ nm), there is a good linear relationship between the difference of fluorescence intensity in the presence of "F" and absence of "F_0" for the pathogenic bacteria *P. aeruginosa* (Fig. 2E), and *S. aureus* (Fig. 2F). Limits of detection of the two bacteria are 2×10^2 and 1.5×10^2 cfu mL^{-1}, respectively. Dynamic linear range, regression and analytical parameters are tabulated in Table 1. Quantum dots (QDs) offer higher sensitivity compared with other conventional methods.[76] However, the autofluorescence of bacteria can be used to detect the bacteria; it is extremely difficult to detect complex biological samples such as bacteria due to biomolecule interferences such as proteins which have also intrinsic fluorescence (*via* aromatic amino acids). Furthermore, there are many drawbacks such as background signals due to impurities in the samples, emission from optical components, scattered light at the incident wavelength, and dark current from the detector. Thus, a reference fluorophore such as CdS@CTS QDs is necessary to circumvent these drawbacks. Semiconductor QDs fluorophores can reduce the autofluorescence of plague cells as they have longer fluorescence lifetimes than cell autofluorescence. Thus, it can drastically reduce the common background signals emitted from biological samples which may undergo overlapping and complicate the spectra. Recently, in order to attenuate the autofluorescence of the chitosan microparticles, Forry *et al.* encapsulated nanoparticles of carbon black (nominal size 12 nm) in order to isolate rare cells, such as circulating tumor cells (CTCs), from a sample of whole blood.[77] Direct measurements of bacteria fluorescence sometimes take place at short

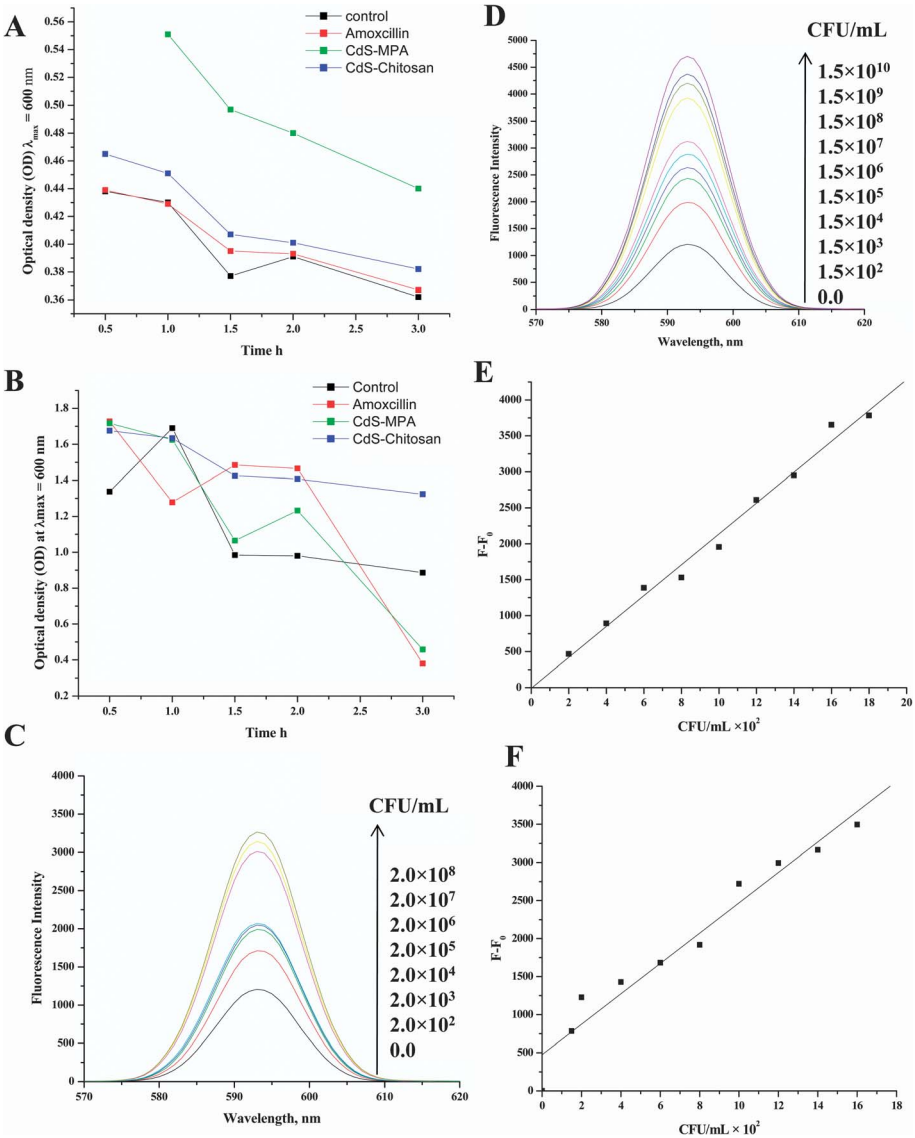

Fig. 2 Optical density of quantum dots and amoxicillin with *P. aeruginosa* (A) and *S. aureus* (B), fluorescence intensity response of CdS@CTS upon addition of different colony forming units of *P. aeruginosa* (C) and *S. aureus* (D) that show a linear relationship (E and F), respectively. Scatter plot of Stern–Volmer of (E) *P. aeruginosa* and (F) *S. aureus*.

Table 1 Analytical parameters of fluorescence emission of chitosan–CdS with the two bacteria

	P. aeruginosa	*S. aureus*
Limit of detection (cfu mL^{-1})	2.0×10^2	1.5×10^2
Linear dynamic range (cfu mL^{-1})	2.0×10^2 to 8.0×10^2	1.5×10^2 to 11.0×10^2
Regression	0.99365	0.97942

excitation wavelength (λ_{ex}) which may cause bacteria death due to the high energy of the laser radiation. Thus, high wavelength is preferable. QDs emission is independent of excitation wavelength,[25] so that samples can be stained with QDs emitting at lower energies than the autofluorescence. We investigate two different excitation wavelengths (360 and 400 nm) as shown in Fig. 3A–D for *P. aeruginosa* and Fig. 4A–D for *S. aureus*, respectively. At the two wavelengths, good linear relationships were recorded in both bacteria (Fig. 3B and D and Fig. 4B and D). CdS@CTS QDs exhibit a wide range of size-tunable colors and independent excitation wavelengths.[25,78,79] The main advantage of the two wavelengths is the low probability of bacteria death as laser energy is considered lower than the CdS excitation wavelength (*i.e.*, 295 nm). Fortunately, there is no effect of the linearity of *P. aeruginosa* (Fig. 3B and D) and for *S. aureus* (Fig. 4B and D). In contrast, the linearity can be improved as the regression values of the Fig. 3 and 4. The design of the nanosensor at high excitation wavelength circumvents the probability of bacteria toxicity by nanomaterials.

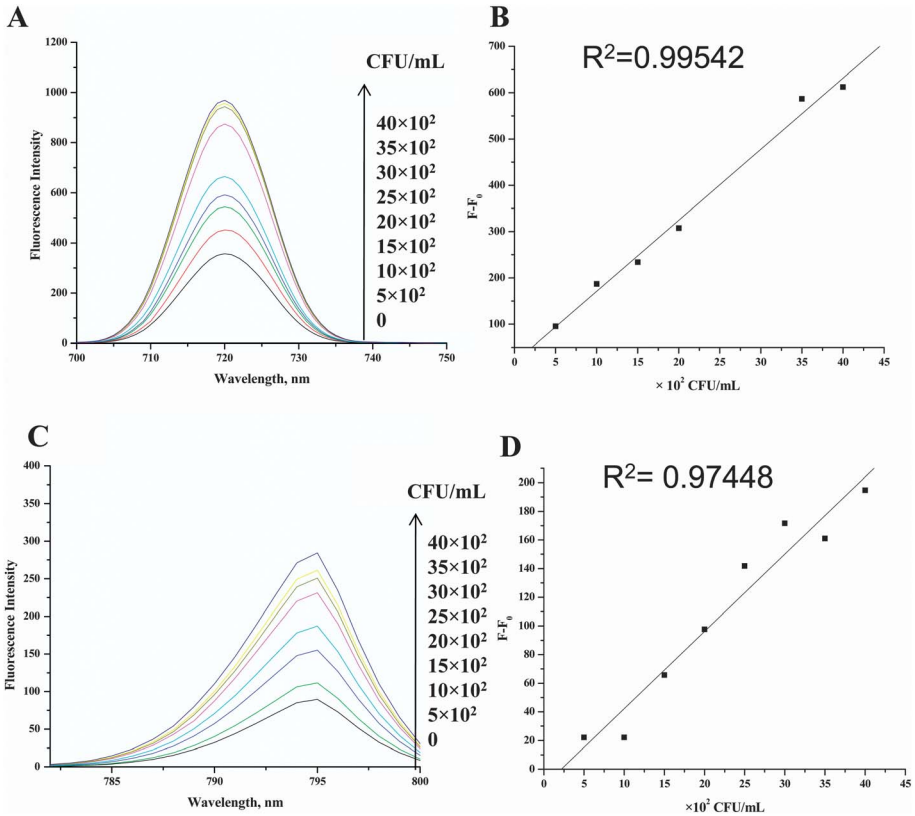

Fig. 3 Fluorescence intensity changes of CdS@chitosan (CdS@CTS) upon addition of different colony forming units of *P. aeruginosa* at 360 nm (A) and 400 nm (B). Linear relationship of fluorescence difference with cfu mL^{-1} of *P. aeruginosa* at 360 nm (C) and 400 nm (D).

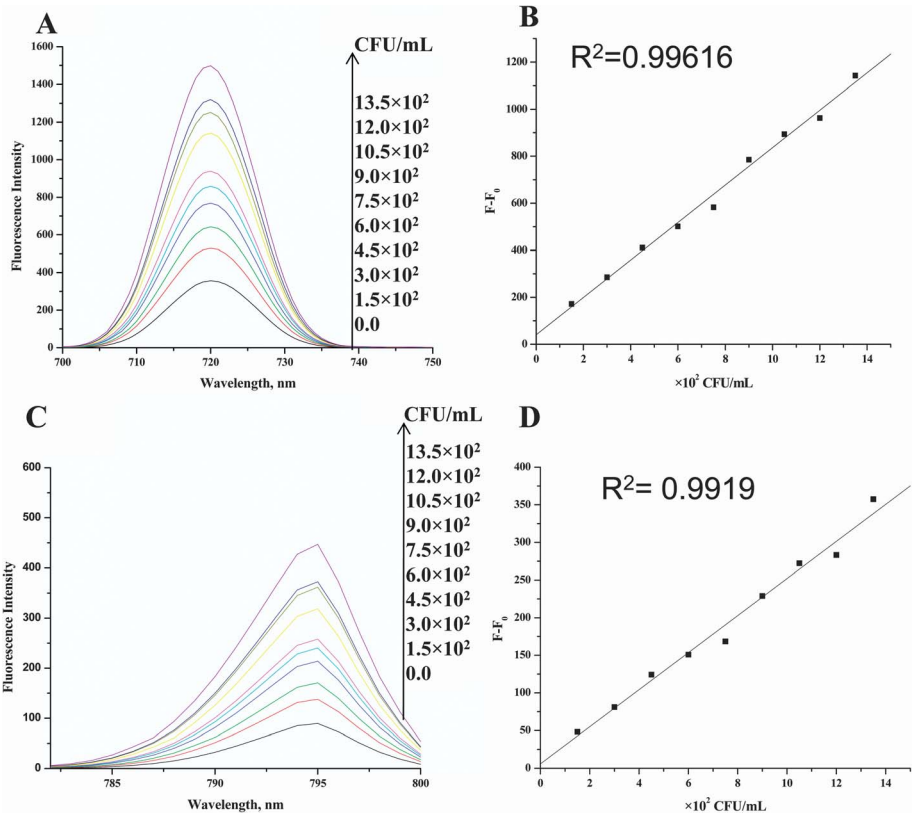

Fig. 4 Fluorescence intensity changes of CdS@CTS upon addition of different colony forming units of *S. aureus* at 360 nm (A) and 400 nm (B). Linear relationship of fluorescence difference with cfu mL^{-1} of *S. aureus* at 360 nm (C) and 400 nm (D).

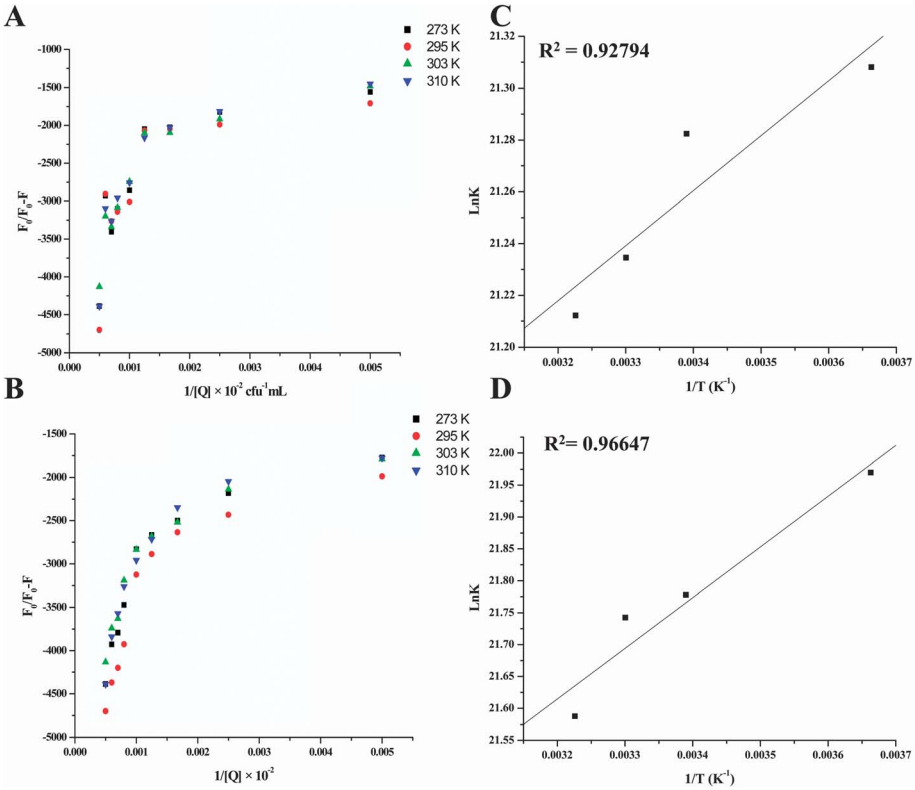

Fig. 5 Van't Hoff plots of the CdS@CTS–*P. aeruginosa* (A) and *S. aureus* (B), scatter plot of Stern–Volmer of *P. aeruginosa* (C) and *S. aureus* (D).

Characterization of the interaction between CdS@CTS QDs and bacteria cell membranes

The interaction of the CdS@CTS with the membrane of pathogenic bacteria can be understood by thermodynamic studies. Unlike ref. 78, there is no shift in the wavelength of QDs@CTS upon binding to bacterial cells that implies the interactions are mainly non-covalent. Kloepfer *et al.*[78] discovered that QDs would be outside the bacteria cell or they would be able to pass though bacterial cell walls that depend on the capping agents. To evaluate the forces which govern the interactions, the thermodynamic analysis is investigated. Generally, chitosan is de-acetylation copolymer of chitin[80] which has similar chemical structures to the bacteria membranes. This copolymer is insoluble in aqueous water, so the aqueous acetic acid (1%) is used to create polycationic QDs.[81–85] There are essentially four types of non-covalent interactions that can play an important role in the interactions among the bacteria membranes and the CdS@CTS system; such as hydrogen bond, van der Waals force, electrostatic, and hydrophobic interaction force. Prior to evaluating the main force, data are recorded at different temperatures (273, 295, 303, and 310 K). Binding constants are investigated using the modified Stern–Volmer as in eqn (2):

$$F_0/(F_0 - F) = 1/fK[Q] + 1/f \quad (2)$$

Table 2 Binding constants for the interaction of CdS@CTS and bacteria

	Binding constant $K \times 10^5$ M^{-1}	
Temp. (K)	*P. aeruginosa*	*S. aureus*
273	5.9	7.5
295	5.4	8.3
303	5.5	6.5
310	5.3	7.4

Table 3 Thermodynamic parameters for the interaction of CdS@CTS and pathogen bacteria

	ΔH^0 (kJ mol^{-1})		ΔS^0 (J mol^{-1} K^{-1})		ΔG^0 (kJ mol^{-1})	
Temp. (K)	*P. aeruginosa*	*S. aureus*	*P. aeruginosa*	*S. aureus*	*P. aeruginosa*	*S. aureus*
273	−1.85	−2.68	103.50	103.39	−30.10	−30.90
295					−32.40	−33.18
303					−33.21	−34.01
310					−33.94	−34.73

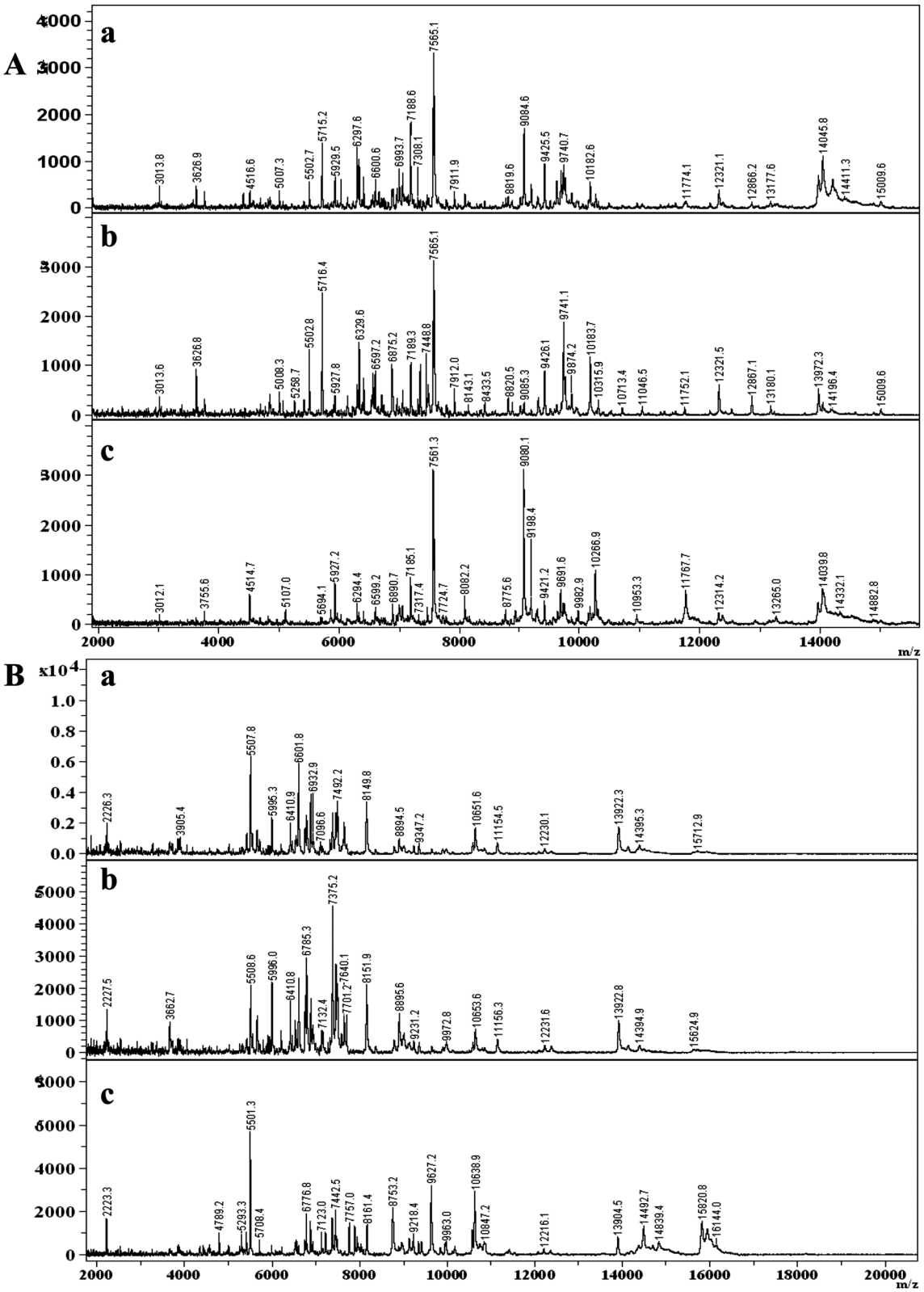

Fig. 6 MALDI-MS spectra of *P. aeruginosa* (A) and *S. aureus* (B) interaction in absence (a) and presence of (b) CdS@MPA and (c) CdS@CTS.

The relationship of $F_0/F_0 - F$ against 1/[Q] at different temperature (273, 295, 303, and 310 K), of *P. aeruginosa* (Fig. 5A) and *S. aureus* (Fig. 5B) present sigmoidal curves. The curve shows a dramatic increase of the intensity until all CdS@CTS bind to bacteria cells, then a plateau is observed. The values of binding constants were calculated and tabulated in Table 2. The results in Table 2 show more strong binding affinity of CdS@CTS toward *S. aureus* than that of

P. aeruginosa. The high affinity features are attributed to the peptidoglycan membrane layers of the pathogenic bacteria. The Gram positive (*S. aureus*) bacteria contain a thick hydrophobic layer than the Gram negative bacteria (*P. aeruginosa*). Thus, this may be the reason for the high affinity with the CdS@CTS QDs. To further understand the mechanisms on the nature of interactions among QDs and bacteria cell membranes, the thermodynamic parameters such as enthalpy change (ΔH^0) and entropy change (ΔS^0), were calculated. The ΔH^0 and ΔS^0 can be determined from the van't Hoff equation as shown in eqn (3):

$$\ln K = -\Delta H^0/RT + \Delta S^0/R \quad (3)$$

where K is the binding constant at the corresponding temperature, R is the gas constant, T is absolute temperature, and ΔH^0 and ΔS^0 are enthalpy and entropy change, respectively. The value of ΔH^0 and ΔS^0 can be obtained from the linear relationship between ln K and the reciprocal absolute temperature (Fig. 5C and D) of *P. aeruginosa* and *S. aureus*, respectively, and the free energy change (ΔG^0) can be obtained from the relationship in eqn (4):

$$\Delta G^0 = \Delta H^0 - T\Delta S^0 \quad (4)$$

The results of the thermodynamic parameters (ΔH^0, ΔS^0, and ΔG^0) are listed in Table 3. From Table 3, it can be seen that ΔH^0 are small negative values. The enthalpy change (ΔH^0) is not significant, while the ΔS^0 values are positive. The negative sign on ΔG^0 indicates the interactions of bacteria membranes to QD@CTS QDs are entropically driven, and the binding processes are spontaneous. While the ΔH^0 changes were small negative values, so the main source of the negative ΔG^0 value comes from the positive value of ΔS^0, thus the main interaction

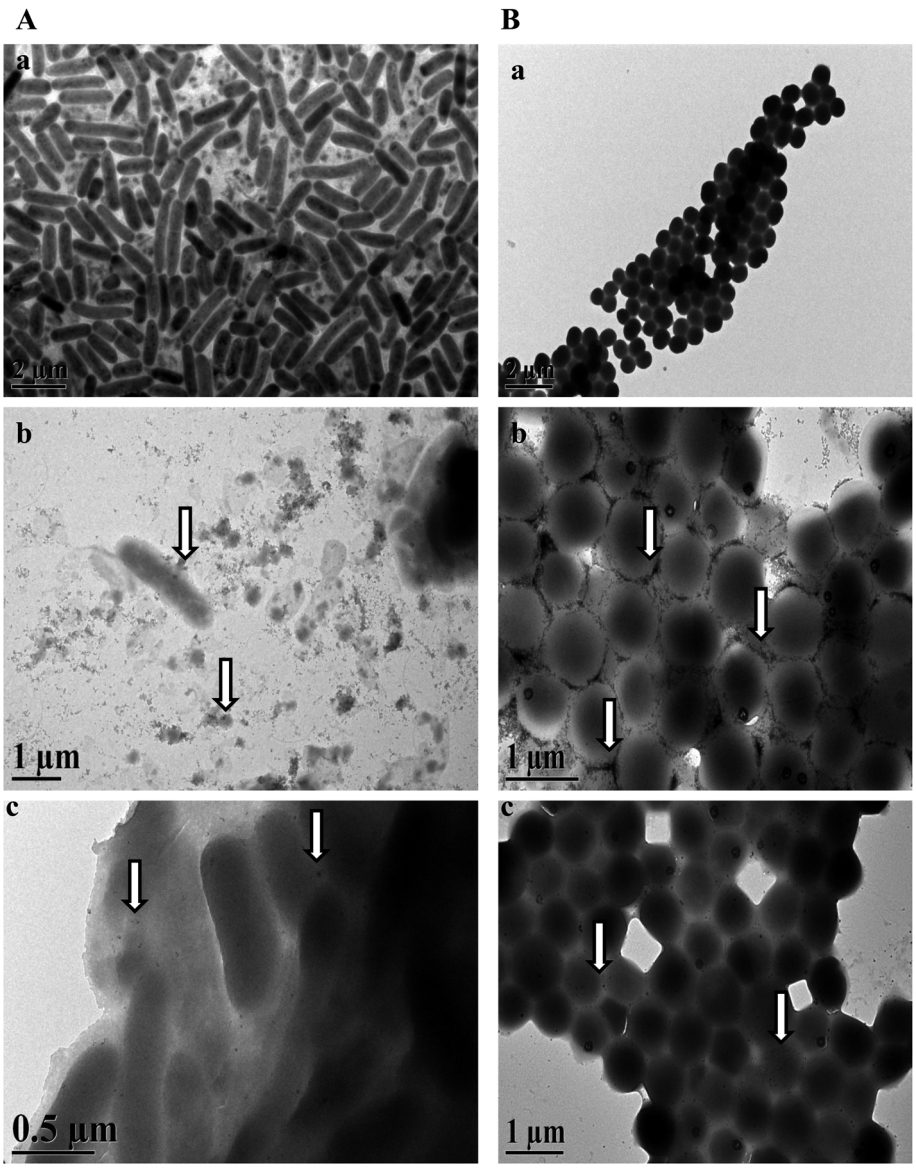

Fig. 7 TEM images of (A) *P. aeruginosa* and (B) *S. aureus* after incubation with (a) control, (b) CdS@MPA and (c) CdS@CTS.

was hydrophobic interaction. At the same time, the small negative value of ΔH^0 indicates hydrogen bonding. From previous observation, we successfully separated the endotoxin of pathogenic bacteria from urine samples using chitosan nanomagnetic particles.[86] Furthermore, there are electrostatic forces between the negative charges of the bacteria and polycationic sites of chitosan. In conclusion, chitosan has multifunctional forces on bacteria (hydrophobic, hydrogen bond, and electrostatic interactions). These forces are complementary and they can reinforce each other. Probing the interactions among biomolecules and pathogenic bacteria is important for separation, biosensing and nanobiomedicine applications.[86,87]

In order to gain a more thorough insight into interactions among CdS@CTS and bacteria cell membrane, we performed matrix assisted laser desorption/ionization mass spectrometry (MALDI-MS) of the bacteria cell before and after incubation. MALDI-MS can be applied for fast monitoring of the interactions among bacteria and QD@CTS. Bacteria cells have fast respond to the environment changes.[48,50] MALDI-MS of *P. aeruginosa* (Fig. 6A) and *S. aureus* (Fig. 6B) after incubation with QDs were investigated. MALDI spectra revealed an increase in the peaks number in the case of CdS@MPA than CdS@CTS. The increase in the peak number indicates degradation of bacteria membranes in the cases of CdS@MPA QDs. While CdS@CTS QDs reveal suppression in the MALDI-MS intensity with negligible change in peak number due to the interactions of CdS@CTS with the cell membranes. Given the limits of the thermodynamic approach and MALDI-MS, the CdS@CTS interaction with the two different bacteria (*P. aeruginosa* and *S. aureus*) has been further investigated by TEM. TEM images were performed to evaluate the CdS@CTS interactions with different bacteria (*P. aeruginosa* (Fig. 7A) and *S. aureus* (Fig. 7B)). The QDs modified with MPA as a capping agent were used and it was found that the nanoparticles actually adhered to the surface of *S. aureus* (Fig. 7B). TEM images show that CdS@MPA circulates *S. aureus*. While, it ruptures *P. aeruginosa* cells (Fig. 7A) which implies high cytotoxicity. In contrast, CdS@CTS shows no or negligible effect on the morphology of pathogenic bacteria cells (Fig. 7) that implies biocompatibility and affinity toward cell membrane. The image displays aggregation of bacteria cells that support the mechanism that we proposed, *i.e.*, "aggregation induced emission enhancement AIEE". MALDI-MS (Fig. 6) and TEM images (Fig. 7) confirm the interactions among QDs and bacteria cell membranes. The CdS@CTS biosensor is crucial for precise intracellular: subcellular bacteria detection and it provides many advantages such as high resolution, high sensitivity, and fast responses for pathogenic bacteria detection.

CdS@CTS provides an ultrafast, biocompatible and sensitive nano-biosensor for broad bacteria. Moreover, we compared our results with the major data on quantum dots capped with different biomolecules to detect bacteria and tabulated the results in Table 4.[43,86–89] Although the immuno-quantum dots, aptamer-QDs, immune-magnetic nanoparticles show selective detection, it is expensive and can inhibit the cell growth. The detection tests using the immuno-QDs typically take a long time (several hours) and the fluorescence signals are easy to be affected by solution pH and the size of quantum dots,[41] pH dependent and are also time consuming. The emission peaks were shifted with increase in the number of bound bacteria;[41] thus quantification is a tedious task. As biological samples are complicated, the magnetic nanoparticles capped with antibody were used to separate pathogenic bacteria before labelling with the antibody-QDs.[42,85] Quantum dots capped with chitosan and immunoglobulin G (QDs–CMCS–IgG) was used to label the bacteria for fluorescence microscopy.[89] However, it was selective, but it shows limitations as it requires centrifugation, and incubation for at least 30 min. Furthermore, it is for identification purpose by using the fluorescence microscopy.[89] The comparison in Table 4 reveals that the CdS@CTS is an ultrafast, sensitive and cheap nano-biosensor compared with reported methods.[40,42,86–88] In most of the conventional techniques, the accurate bacteria cells number can only be obtained after the bacteria are cultured, hence, the adjustment of cultivation parameters depends solely on experience and large amounts of experiments.[19–23] It needs at least 2–8 days to obtain confirmed results and lacks high sensitivity.[19–23] Thus, it is important to develop an effective biosensor that can generate photoluminescence changes as a function of the bacteria cells numbers such as here. From these results we can conclude that CdS@CTS QDs exhibit high potential to be applied as effective biosensors for detecting pathogenic bacteria.

Table 4 Comparison between different quantum dots which were proposed for bacteria[a]

QDs	Bacteria	LOD (cfu mL^{-1})	Range (cfu mL^{-1})	Time	Ref.
Quantum dot biolabeling coupled with immunomagnetic separation	*E. coli* O157:H7	10^3	10^3 to 10^7	<2 h	83
CdSeQDs@TGA	*E. coli* and *S. aureus*	10^2	10^2 to 10^7	1–2 h	40
Qdot-525 streptavidin conjugate	*Escherichia coli* O157:H7 and *Salmonella Typhimurium*	10^4	ND	2 h	42
Mannose-coated CdS quantum dots (Man-QDs)	*Escherichia coli*	10^4	ND	>1 h	87
QDs–CMCS–IgG	*S. aureus*	900	10^3 to 10^7	>40 min	88
QDs@CTS	*S. aureus* and *P. aeruginosa*	150–200	1.5×10^2 to 18.0×10^2	1 min	Here

[a] Abbreviation: carboxymethyl chitosan; CdS CMCS, ND; not detected, thioglycolic acid; TGA, immunoglobulin G; IgG, chitosan; CTS, mannose; Man, hour; h, minute; min.

Conclusion

The blue emission of CdS@chitosan (CdS@CTS) displays fluorescence enhancement as a function of the pathogenic bacteria colonies (*S. aureus*, *P. aeruginosa*) at extremely low detection limits (150 and 200 cfu mL^{-1}) and wide linear dynamic range. The CdS@CTS QDs offer many advantages, as it is an ultrafast, highly sensitive, stable (for a long time), label free (direct) detection with good biocompatibility. A dose–response and calibration curve shows that the CdS@CTS QD is sensitive in relevant concentration range. In our experiments, the negative ΔH for the interactions between CdS@CTS and bacteria cells for the first binding event indicated that the hydrophobic interactions play a key role in the first binding reaction due to the positive values of ΔS, while electrostatic and hydrogen bonding interactions were deduced for the second binding event. The strong binding affinity of CdS@CTS toward *S. aureus* than *P. aeruginosa* is attributed to the peptidoglycan membrane layers of the pathogenic bacteria. The current CdS@CTS QD approach exhibits excellent and unique features to be applied as a superior biosensor for a variety of applications. The interactions have been confirmed with MALDI-MS and TEM images.

Acknowledgements

We thank the National Science Council of Taiwan for financial support. Mr Khan (doctoral program in marine biotechnology), National Sun Yat-Sen University, Taiwan, is acknowledged for his help on the plate counting protocols. We also thank Mr Kuo Chiang Wang for help with the TEM microscopy studies.

References

1 P. A. Alivisatos, *J. Phys. Chem.*, 1996, **100**, 13226–13239.
2 J. Che, X. Wang, Y. Xiao, X. Wu, L. Zhou and W. Yuan, *Nanotechnology*, 2007, **18**, 135706.
3 N. H. Alsharif, C. E. M. Berger, S. S. Varanasi, Y. Chao, B. R. Horrocks and H. K. Datta, *Small*, 2009, **5**, 221–228.
4 J. Li and J.-J. Zhu, *Analyst*, 2013, **138**, 2506–2515.
5 J. H. Warner and R. D. Tilley, *Nanotechnology*, 2006, **17**, 3745–3749.
6 M. Nirmal, B. O. Dabbousi, M. G. Bawendi, J. J. Macklin, J. K. Trautman, T. D. Harris and L. E. Brus, *Nature*, 1996, **383**, 802–804.
7 T. Jamieson, R. Bakhshi, D. Petrova, R. Pocock, M. Imani and A. M. Seifalian, *Biomaterials*, 2007, **28**, 4717–4732.
8 X. Luo, A. Morrin, A. J. Killard and M. R. Smyth, Application of nanoparticles in electrochemical sensors and biosensors, *Electroanalysis*, 2006, **18**, 319–326.
9 J. Shi, Y. Zhu, X. Zhang, W. R. G. Baeyens and A. M. Garcia-Campana, *TrAC, Trends Anal. Chem.*, 2004, **23**, 351–360.
10 P. Wu and X. P. Yan, Doped quantum dots for chemo/biosensing and bioimaging, *Chem. Soc. Rev.*, 2013, **42**, 5489–5521.
11 I. Willner, R. Baron and B. Willner, *Biosens. Bioelectron.*, 2007, **22**, 1841–1852.
12 L. E. Brus, *J. Chem. Phys.*, 1983, **79**, 5566–5571.
13 Z. L. Wang, *Characterization of Nanophase Materials*, Wiley-VCH Verlag GmbH, Weinheim, 1st edn, 2000.
14 A. Hagfeldt and M. Gratzel, *Chem. Rev.*, 1995, **95**, 49–68.
15 C. Burda, T. C. Green, S. Link and M. A. El-Sayed, *J. Phys. Chem. B*, 1999, **103**, 1783–1788.
16 C. Landes, C. Burda, M. Braun and M. A. El-Sayed, *J. Phys. Chem. B*, 2001, **105**, 2981–2986.
17 C. A. Suchetti, R. H. Lema and M. Hamity, *J. Photochem. Photobiol., A*, 2005, **169**, 1–8.
18 A. Hasselbarth, A. Eychmueller and H. Weller, *Chem. Phys. Lett.*, 1993, **203**, 271–276.
19 D. Ivnitski, I. Abdel-Hamid, P. Atanasov and E. Wilkins, *Biosens. Bioelectron.*, 1999, **14**, 599–624.
20 A. P. F. Turner, M. F. Cardosi, G. Ramsay, B. H. Schneider and A. Swain, Biosensors for use in the food industry: a new rapid bioactivity monitor, in *Biotechnology in the Food Industry*, Online Publications, Pinner UK, 1986, pp. 97–116.
21 M. Tietjen and D. Y. C. Fung, *Crit. Rev. Microbiol.*, 1995, **21**, 53–83.
22 J. R. Lakowicx, *Principle of Fluorescence spectroscopy*, Spring Science & Business Media, New York, 3rd edn, 2006.
23 T. M. Rossi and M. Warner, Bacterial identification using fluorescence spectroscopy, in *Instrumental Methods for Rapid Microbiological Analysis*, ed. W. H. Nelson, VCH Publishers, 1985, ch. 1, pp. 1–50.
24 E. Harlow and D. Lane, *Using Antibodies: A Laboratory Manual*, Cold Spring harbor Laboratory Press, NY, 1999.
25 M. Bruchez, M. Moronne, P. Gin, S. Weiss and A. P. Alivisatos, *Science*, 1998, **281**, 2013–2016.
26 C. A. Leatherdale, W. K. Woo, F. V. Mikulec and M. G. Bawendi, *J. Phys. Chem. B*, 2002, **106**, 7619–7622.
27 W. W. Yu, L. Qu, W. Guo and X. Peng, *Chem. Mater.*, 2003, **15**, 2854–2860.
28 A. Striolo, J. Ward, J. M. Prausnitz, W. J. Parak, D. Zanchet, D. Gerion, D. Milliron and A. P. Alivisatos, *J. Phys. Chem. B*, 2002, **106**, 5500–5505.
29 O. Schmelz, A. Mews, T. Basche, A. Herrmann and K. Mullen, *Langmuir*, 2001, **17**, 2861–2865.
30 W. C. W. Chan and S. Nie, *Science*, 1998, **281**, 2016–2018.
31 B. Dubertret, P. Skourides, D. J. Norris, V. Noireaux, A. H. Brivanlou and A. Libchaber, *Science*, 2002, **298**, 1759–1762.
32 S. Pathak, S. K. Choi, N. Arnheim and M. E. Thompson, *J. Am. Chem. Soc.*, 2001, **123**, 4103–4104.
33 J. O. Winter, T. Y. Liu, B. A. Korgel and C. E. Schmidt, *Adv. Mater.*, 2001, **13**, 1673–1677.
34 S. J. Rosenthal, I. Tomlinson, E. M. Adkins, S. Schroeter, S. Adams, L. Swafford, J. McBride, Y. Wang, L. J. DeFelice and R. D. Blakely, *J. Am. Chem. Soc.*, 2002, **124**, 4586–4594.
35 D. Ishii, K. Kinbara, Y. Ishida, N. Ishii, M. Okochi, M. Yohda and T. Aida, *Nature*, 2003, **423**, 628–632.
36 S. Wang, N. Mamedova, N. A. Kotov, W. Chen and J. Studer, *Nano Lett.*, 2002, **2**, 817–822.
37 M. Dahan, S. Levi, C. Luccardini, P. Rostaing, B. Riveau and A. Triller, *Science*, 2003, **302**, 442–445.
38 J. Gao, L. Li, P. L. Ho, G. C. Mak, H. Gu and B. Xu, *Adv. Mater.*, 2006, **18**, 3145.

39 S. Ryan, A. J. Kell, H. Van Faassen, L. L. Tay, B. Simard and R. MacKenzie, *Bioconjugate Chem.*, 2009, **20**, 1966–1974.
40 X. Xue, I. Pan, H. Xie, J. Wang and S. Zhang, *Talanta*, 2009, **77**, 1808–1813.
41 S. Dwarakanatha, J. G. Brunob, A. Shastrya, T. Phillipsb, A. Johnc, A. Kumarc and L. D. Stephenson, *Biochem. Biophys. Res. Commun.*, 2004, **325**, 739–743.
42 L. Yang and Y. Li, *Analyst*, 2006, **131**, 394–401.
43 X. L. Su and Y. B. Li, *Anal. Chem.*, 2004, **76**, 4806–4810.
44 L. Yang and Y. Li, *Analyst*, 2006, **131**, 394–401.
45 Y. Otsuka, K.-I. Hanaki, J. Zhao, R. Ohtsuki, K. Toyooka, H. Yoshikura, T. Kuratsuii, K. Yamamoto and T. Kirikae, *Jpn. J. Infect. Dis.*, 2004, **57**, 183–184.
46 N. I. Chalmers, R. J. Palmer, Jr, L. Du-Thumm, R. Sullivan, W. Shi and P. E. Kolenbrander, *Appl. Environ. Microbiol.*, 2007, **73**, 630–636.
47 W. G. Cox and V. L. Singer, Fluorescent DNA hybridization probe preparation using amine modification and reactive dye coupling, *BioTechniques*, 2004, **36**, 114–122.
48 H. N. Abdelhamid and H. F. Wu, *Anal. Chim. Acta*, 2012, **751**, 94–104.
49 H. F. Wu, J. Gopal, H. N. Abdelhamid and N. Hasan, *Proteomics*, 2012, **12**, 2949–2961.
50 H. N. Abdelhamid and H. F. Wu, *J. Mater. Chem. B*, 2013, **1**, 3950–3961.
51 R. Jayakumar, D. Menon, K. Manzoor, S. V. Nair and H. Tamura, *Carbohydr. Polym.*, 2010, **82**, 227–232.
52 S. Lai, X. Chang and C. Fu, *Microchim. Acta*, 2009, **165**, 39–44.
53 Y. Kea, S. K. Kailasa, H. F. Wu and Z. Y. Chen, *Talanta*, 2010, **83**, 178–184.
54 Z. Li, Y. M. Du and Z. L. Zhang, *React. Funct. Polym.*, 2003, **55**, 35–43.
55 H. N. Abdelhamid, J. Gopal and H. F. Wu, *Anal. Chim. Acta*, 2013, **767**, 104–111.
56 W. W. Yu and X. Peng, *Angew. Chem., Int. Ed.*, 2002, **41**, 2368–2371.
57 P. Kolhe and R. M. Kannan, *Biomacromolecules*, 2003, **4**, 173–180.
58 R. Sekar, S. K. Kailasa, H. N. Abdelhamid, Y. C. Chen and H. F. Wu, *Int. J. Mass Spectrom.*, 2013, **338**, 23–29.
59 Y. F. Chen and Z. Rosenzweig, *Nano Lett.*, 2002, **2**, 1299–1302.
60 C. B. Murray, D. J. Norris and M. G. Bawendi, *J. Am. Chem. Soc.*, 1993, **115**, 8706–8715.
61 M. A. Hines and P. Guyot-Sionnest, *J. Phys. Chem.*, 1996, **100**, 468–471.
62 W. C. W. Chan, D. J. Maxwell, X. H. Gao, R. E. Bailey, M. Y. Han and S. M. Nie, *Curr. Opin. Biotechnol.*, 2002, **13**, 40–46.
63 P. O'Brien, S. S. Cummins, D. Darcy, A. Dearden, M. Ombaretta, N. L. Pickett, S. Ryley and A. J. Sutherland, *Chem. Commun.*, 2003, 2532–2533.
64 W. B. Tan, N. Huang and Y. Zhang, *J. Colloid Interface Sci.*, 2007, **310**, 464–470.
65 H. N. Abdelhamid and H. F. Wu, *Talanta*, 2013, **115**, 442–444.
66 R. A. Hardman, *Environ. Health Perspect.*, 2006, **114**, 165–172.
67 A. Hoshino, K. Hanaki, K. Suzuki and K. Yamamoto, *Biochem. Biophys. Res. Commun.*, 2004, **314**, 46–53.
68 A. M. Derfus, W. C. W. Chan and S. N. Bhatia, *Nano Lett.*, 2004, **4**, 11–14.
69 G. Gedda, J. Gopal and H. F. Wu, *Rapid Commun. Mass Spectrom.*, 2012, **30**, 1609–1616.
70 H. F. Bao, N. Hao, Y. Yang and D. Zhao, *Nano Res.*, 2010, **3**, 481–489.
71 M. Bottrill and M. Green, *Chem. Commun.*, 2011, **47**, 7039–7050.
72 Y. Li, Y. L. Zhou, H. Y. Wang, S. Perrett, Y. L. Zhao, Z. Y. Tang and G. J. Nie, *Angew. Chem., Int. Ed.*, 2011, **50**, 5860–5864.
73 M. T. Cook, G. Tzortzis, V. V. Khutoryanskiy and D. Charalampopoulos, *J. Mater. Chem. B*, 2013, **1**, 52–73.
74 L. Marin, I. Stoica, M. Mares, V. Dinu, B. C. Simionescu and M. Barboiu, *J. Mater. Chem. B*, 2013, **1**, 3353–3358.
75 I. Perelshtein, E. Ruderman, N. Perkas, T. Tzanov, J. Beddow, E. Eadaoin Joyce, T. J. Mason, M. Blanes, K. Molla, A. Patlolla, A. I. Frenkele and A. Gedanken, *J. Mater. Chem. B*, 2013, **1**, 1968–1976.
76 M. A. Hahn, J. S. Tabb and T. D. Krauss, *Anal. Chem.*, 2005, **77**, 4861–4869.
77 C. Arya, J. G. Kralj, K. Jiang, M. S. Munson, T. P. Forbes, D. L. DeVoe, S. R. Raghavan and S. P. Forry, *J. Mater. Chem. B*, 2013, **1**, 4313–4319.
78 J. A. Kloepfer, R. E. Mielke, M. S. Wong, K. H. Nealson, G. Stucky and J. L. Nadeau, *Appl. Environ. Microbiol.*, 2003, **69**, 4205–4213.
79 E. M. Boatman, G. C. Lisensky and K. J. Nordell, *J. Chem. Educ.*, 2005, **82**, 1697–1699.
80 H. Li, L. Q. Wu, W. E. Bentley, R. Ghodssi, G. W. Rubloff, J. N. Culver and J. G. P. Payne, *Biomacromolecules*, 2005, **6**, 2881–2894.
81 M. Rinaudo, G. Pavlov and J. Desbrieres, *Polymer*, 1999, **40**, 7029–7032.
82 P. Sorlier, A. Denuziere, C. Viton and A. Domard, *Biomacromolecules*, 2001, **2**, 765–772.
83 S. P. Strand, K. Tommeraas, K. M. Varum and K. Ostgaard, *Biomacromolecules*, 2001, **2**, 1310–1314.
84 M. W. Anthonsen and O. Smidsrod, *Carbohydr. Polym.*, 1995, **26**, 303–305.
85 K. M. Varum, M. H. Ottoy and O. Smidsrod, *Carbohydr. Polym.*, 1994, **25**, 65–70.
86 J. Gopal, H. N. Abdelhamid, P. Y. Hua and H. F. Wu, *J. Mater. Chem. B*, 2013, **1**, 2463–2475.
87 H. N. Abdelhamid, Applications of nanomaterials and organic semiconductors for bacteria & biomolecules analysis/biosensing using laser analytical spectroscopy, Master's thesis, National Sun-Yat Sen university, 2013, etd-0608113–135030.
88 B. Mukhopadhyay, M. B. Martins, R. Karamanska, D. A. Russell and A. Robert, *Tetrahedron Lett.*, 2009, **50**, 886–889.
89 X. Wang, Y. Du, Y. Li, D. Li and R. Sun, *J. Biomater. Sci., Polym. Ed.*, 2011, **22**, 1881–1893.

